

Noise-induced cooperative dynamics and its control in coupled neuron models

B. Hauschildt,^{1,*} N. B. Janson,^{2,†} A. Balanov,^{1,3,‡} and E. Schöll^{1,§}

¹*Institut für Theoretische Physik, Technische Universität Berlin, Hardenbergstrasse 36, D-10623 Berlin, Germany*

²*Department of Mathematical Sciences, Loughborough University, Loughborough, Leicestershire, LE11 3TU, United Kingdom*

³*School of Physics and Astronomy, University of Nottingham, University Park, Nottingham, NG7 2RD, United Kingdom*

(Received 17 April 2006; revised manuscript received 13 September 2006; published 8 November 2006)

We investigate feedback control of the cooperative dynamics of two coupled neural oscillators that is induced merely by external noise. The interacting neurons are modeled as FitzHugh-Nagumo systems with parameter values at which no autonomous oscillations occur, and each unit is forced by its own source of random fluctuations. Application of delayed feedback to only one of two subsystems is shown to be able to change coherence and time scales of noise-induced oscillations either in the given subsystem, or globally. It is also able to induce or to suppress stochastic synchronization under certain conditions.

DOI: [10.1103/PhysRevE.74.051906](https://doi.org/10.1103/PhysRevE.74.051906)

PACS number(s): 87.19.La

I. INTRODUCTION

Neural systems in many cases are characterized by oscillatory behavior [1–3], which is often quite complicated [4]. It has been shown that neural oscillatory dynamics can have different origins, being either self-sustained [5], or induced by random fluctuations alone [6,7]. These oscillations can also be multimodal, i.e., consisting of several components with different prominent time scales. For example, the thalamocortical relay neurons can generate either spindle or δ oscillations [8], whereas the electroreceptors in a paddle fish are able to generate biperiodic oscillations [9]. Coupled neurons are able to demonstrate synchronization, which plays a very important role in neurodynamics, having either constructive or destructive effects depending on the circumstances.

On one hand, the ensembles of different neurons can be synchronized in order to process biological information, i.e., this synchronization might be beneficial for a more efficient data transmission [10,11]. On the other hand, these synchronized neurons can induce a regular, rhythmic activity, which is believed to play a crucial role in the emergence of pathological rhythmic brain activity in Parkinson's disease, essential tremor, and epilepsy [12,13]. In both situations, synchronization phenomena occur spontaneously, and the mechanisms behind them are the subjects of intensive research [11,13]. Hence, the development of techniques that would allow one to manipulate the neural synchrony is an important clinical problem.

Starting with the work of Ott, Grebogi, and Yorke [14], a variety of methods for the control of irregular behavior have been developed in the last 15 years [15,16]. Recently, a number of methods have been proposed for suppression of synchrony in the arrays of coupled oscillators in which oscillations are self-sustained [17,18]. However, the problem of control of the dynamics in coupled systems where oscilla-

tions are induced merely by random fluctuations is still open.

In this paper we investigate the possibility of using for this purpose the delayed feedback scheme introduced by Pyragas [19]: it constructs a control force from the difference between the current state of the system and its state some τ time units ago. This method is known as *time-delay autosynchronization* (TDAS). It has been applied to control of deterministic chaos in a wide range of systems including spatially extended models, e.g., [20–22]. It was also demonstrated that it can be used to control the coherence and the time scales of noise-induced oscillations in a single system [23–25]. This theoretical prediction has recently been verified experimentally in an electrochemical oscillator system [26]. The main aim of the present work is to extend time-delayed feedback control of noise-induced dynamics to *coupled* excitable systems, and investigate if *local* control applied to a subsystem can allow one to steer the *global* cooperative dynamics in a system of coupled neural oscillators. In particular, we are interested in the study of the effects of delayed feedback on the *synchrony* properties in coupled neuron systems.

The paper is organized as follows. In Sec. II we introduce the model system used, and discuss the properties of their cooperative behavior without control. In Sec. III we study the effects of local delayed feedback control on the global behavior of coupled systems. In Sec. IV the results are summarized and the conclusions are drawn.

II. GLOBAL DYNAMICS OF TWO COUPLED NEURAL OSCILLATORS

In order to grasp the complicated interaction between 10^9 of neurons in large neural networks, those are often lumped into groups of neural populations each of which can be represented as an effective excitable element that is mutually coupled to the other elements [17,18]. In this sense the simplest model which may reveal features of interacting neurons consists of two coupled neural oscillators. Each of these can be represented by, e.g., a simplified FitzHugh-Nagumo system, which is often used as a paradigmatic generic model for neurons, or more generally, excitable systems [27]. Here we use two FitzHugh-Nagumo systems with substantially differ-

*Electronic address: hauschildt@nlds.physik.tu-berlin.de

†Electronic address: n.b.janson@lboro.ac.uk

‡Electronic address: alexander.balanov@nottingham.ac.uk

§Electronic address: schoell@physik.tu-berlin.de

ent intrinsic time scales, and parameters corresponding to the excitable regime.

Before attempting to control their global dynamics with locally applied feedback, we will first study the dynamics of the uncontrolled coupled system. The dynamical equations are given by

$$\begin{aligned} \epsilon_1 \dot{x}_1 &= x_1 - \frac{x_1^3}{3} - y_1 + C(x_2 - x_1), \\ \dot{y}_1 &= x_1 + a + D_1 \xi_1(t), \end{aligned} \quad (1)$$

$$\begin{aligned} \epsilon_2 \dot{x}_2 &= x_2 - \frac{x_2^3}{3} - y_2 + C(x_1 - x_2), \\ \dot{y}_2 &= x_2 + a + D_2 \xi_2(t), \end{aligned} \quad (2)$$

where subsystems, Eqs. (1) and (2), represent two different neurons, x_i ($i=1,2$) describing the transmembrane voltages and y_i modeling the behavior of several physical quantities related to electrical conductances of the relevant ion currents across the respective membranes. Here a is a bifurcation parameter whose value defines whether the system is excitable or demonstrates periodic firing (autonomous oscillations), ϵ_1 and ϵ_2 are positive parameters that are usually chosen to be much smaller than unity, ξ_1 and ξ_2 are independent sources of Gaussian white noise with zero mean and unity variance, D_1 and D_2 are noise intensities.

The synaptic coupling between two neurons is modeled as a diffusive coupling considered for simplicity to be symmetric [28–30]. The coupling strength C summarizes how information is distributed between neurons.

We shall restrict our analysis to the range of the parameter values where without noise each of the two subsystems exhibits excitability with only one attractor in the form of a stable fixed point. Noise sources ξ_1 and ξ_2 model random inputs that represent integral signals coming from the part of the neural network or of the environment with which the neuron is connected. Since the neurons can be coupled to different parts of the neural network or of the environment, the noise intensities in the two systems can be quite different.

A. Features of a single neuron model

Let us illustrate the dynamics of a single neuron model by considering an uncoupled subsystem, Eqs. (1) ($C=0$), under the influence of noise. We arbitrarily fix $D_1=0.02$, and also set $a=1.05$, $\epsilon_1=0.005$. In Fig. 1(a) the dashed lines show the null clines of Eq. (1) that intersect at a fixed point marked by a white circle. The phase point that is initially placed at the fixed point stays in its close vicinity if the applied random perturbation remains small. However, if the perturbation is larger than some threshold value, the phase point makes a large excursion in the phase space before returning to the vicinity of the fixed point again. In Fig. 1(a) the black solid line illustrates a phase portrait and in Fig. 1(b) realizations of x_1 and y_1 time series from Eqs. (1) are shown. The motion of the phase point consists of two stages: an activation time during which the system waits for a sufficiently large pertur-

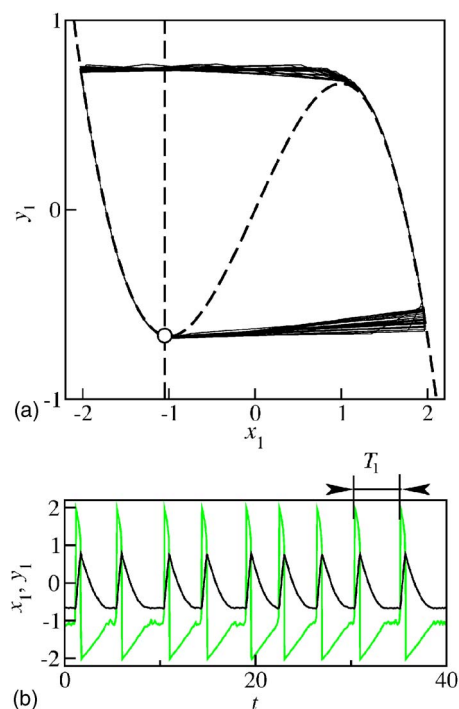


FIG. 1. (Color online) (a) Phase portrait and (b) realizations of x_1 (gray, green online) and y_1 (black) time series in a single FitzHugh-Nagumo system, Eq. (1). In (a) dashed lines are null clines and the fixed point is shown by a white circle. Parameters: $a=1.05$, $\epsilon_1=0.005$, $D_1=0.02$.

bation before it can make an excursion, and the excursion itself. The excursion time is almost completely defined by the deterministic properties of the system and is hardly influenced by noise.

On the contrary, the activation time is completely determined by the properties of noise if all other parameters are fixed: the stronger the noise, the smaller the activation time and the larger the mean frequency of noise-induced oscillations is. Thus, the noise strengths D_1 and D_2 control the average frequencies of noise-induced oscillations in the systems Eqs. (1) and (2), respectively, and the difference between them defines the mean frequency detuning between the systems.

B. Means for characterizing cooperative dynamics

Before studying the effects of delayed feedback control on the model, Eqs. (1) and (2), let us examine the basic features of cooperative dynamics of two systems in which oscillations are induced merely by noise.

The cooperative dynamics of a system of coupled stochastic oscillators can be characterized differently depending on the feature of interest. The most popular features are time scales involved, degree of order in each partial subsystem and in the system of coupled oscillators as a whole, and the degree of synchronism between the subsystems. To quantitatively characterize each feature of interest, a number of criteria can be used, and here we will choose those that seem to suit best our purposes.

Time scales. The Fourier power spectral density, to which in the following we will refer as *spectrum* for brevity, seems to be the most universal and sensitive tool that allows one to fully reveal the frequency content of random oscillations and thus characterize the time scales involved. The central frequencies of the highest spectral peaks will characterize the time scales involved.

Another convenient and less computationally expensive way to characterize the time scales of oscillations is to introduce the interspike intervals (ISI) T_1 and T_2 for the two systems from their realizations $x_1(t)$ and $x_2(t)$, respectively, as shown in Fig. 1(b). The average ISIs $\langle T_i \rangle$, $i=1,2$, will also characterize the time scales of two systems.

Coherence. Generally, the width of the spectral peak can serve as an indication of the coherence of the oscillations: the narrower the peak is, the more coherent the oscillations are. However, as we will see below, the spectra of the observed oscillations have several distinguishable peaks with comparable heights placed at incommensurate frequencies (i.e., at frequencies that are not multiples of each other), and all peaks have different widths. It is not obvious the width of which peak should be taken as a measure of coherence, and thus the peak width does not represent an unambiguous criterion here and will not be used.

Another measure of coherence of oscillations is the correlation time t_{cor} . It is also not unambiguous because it can be introduced in several ways. Here we will use the following method which seems the most universal: an autocorrelation function $\Psi(s) = \langle [x(t-s) - \langle x \rangle][x(t) - \langle x \rangle] \rangle$ will be calculated from the simulated realizations $x(t)$, and t_{cor} will be introduced as

$$t_{cor} = \frac{1}{\sigma^2} \int_0^\infty |\Psi(s)| ds, \quad (3)$$

where $\sigma^2 = \Psi(0)$ is the variance of $x(t)$. The larger t_{cor} is, the more regular $x(t)$ is.

Time scales and coherence can be introduced for each subsystem separately and then compared, or for some variable characterizing the state of the system as a whole. Thus, we will estimate the statistical characteristics of the variables x_1 and x_2 , and of the global state variable $x_\Sigma = x_1 + x_2$.

Synchronization. Finally, we need to characterize the synchronization between the two coupled oscillators. Most generally, synchronization means an adjustment of time scales of oscillations in systems due to the interaction between them: if the time scales in the uncoupled systems are not rationally related, introduction of coupling can shift the time scales to make their ratio closer to a rational number $n:m$, where n and m are integers. This phenomenon is usually referred to as $n:m$ frequency synchronization, and its suitable measure would be the closeness of the ratio of average ISIs $\langle T_1 \rangle / \langle T_2 \rangle$ to the chosen rational number $n:m$. Note that frequency synchronization is associated with the time-averaged behavior of the coupled oscillators.

A closely related, but not identical, phenomenon, which is usually called phase synchronization, is associated with instantaneous coordination between the interacting systems. It requires the definition of phases $\varphi_1(t)$ and $\varphi_2(t)$ for each

oscillator and comparison between them. In our system the spiky nature of oscillations allows one to introduce the phase for each system as

$$\varphi_j(t) = 2\pi \frac{t - t_{i-1}}{t_i - t_{i-1}} + 2\pi(i-1), \quad j=1,2,\dots, \quad (4)$$

where t_i is the time at which we observe a spike in the respective system's realization.

We define $n:m$ phase synchronization to occur if the phase difference

$$\Delta\varphi_{n,m}(t) = \varphi_1(t) - \frac{m}{n}\varphi_2(t) \quad (5)$$

exhibits horizontal plateaus of sufficient duration. Usually, if $n:m$ synchronization takes place, $\Delta\varphi_{n,m}(t)$ demonstrates plateaus occasionally interrupted by 2π jumps. On the plateaus, $\Delta\varphi_{n,m}(t)$ usually oscillates around some local average level. As time grows, $\Delta\varphi_{n,m}(t)$ drifts to plus or minus infinity.

In Ref. [31] several measures to characterize phase synchronization were introduced. Here, we choose to estimate the synchronization index

$$\gamma_{n,m} = \sqrt{\langle \cos \Delta\varphi_{n,m}(t) \rangle^2 + \langle \sin \Delta\varphi_{n,m}(t) \rangle^2}. \quad (6)$$

$\gamma_{n,m}$ can vary between 0 (no synchronization) and 1 (perfect $n:m$ phase synchronization). Note that even if the ratio of average ISIs is close or even equal to some rational number $n:m$, i.e., frequency synchronization takes place, phase synchronization does not necessarily occur, and the synchronization index might be close to zero.

C. Cooperative noise-induced dynamics in two coupled neurons: time scales and coherence

All results in this paper are presented for $a=1.05$, $\epsilon_1=0.005$, $\epsilon_2=0.1$, and $D_2=0.09$. Mean frequency detuning will be determined by the choice of D_1 . Note that $\epsilon_1 \neq \epsilon_2$, i.e., the systems are not identical, therefore at $D_1=D_2$ the mean frequencies of oscillations in two uncoupled ($C=0$) systems will be different.

We need to find out how the cooperative dynamics of the interacting systems changes depending on coupling strength C and on the mean frequency detuning defined by D_1 .

We first fix the coupling strength C at 0.07, and change D_1 . Figure 2 shows the realizations x_1 , x_2 , and x_Σ of noise-induced oscillations. At $D_1=0$ the first subsystem, whose variables are denoted by subscript 1 in Eq. (1), has no independent dynamics. But due to the coupling with the second subsystem, it demonstrates forced oscillations whose properties are completely defined by those of the second subsystem. The respective realizations of x_1 and x_2 demonstrate excellent synchrony, so that each spike in x_2 causes a spike in x_1 that occurs simultaneously [Fig. 2 ($D_1=0$)].

At $D_1 \neq 0$ the first subsystem acquires its own dynamics with the respective independent time scale. Now each time one of the subsystems produces a noise-induced spike, due to coupling the other subsystem is prompted to spike, too: it does not necessarily emit a spike, but the spiking probability grows slightly. As a result, both subsystems are likely to

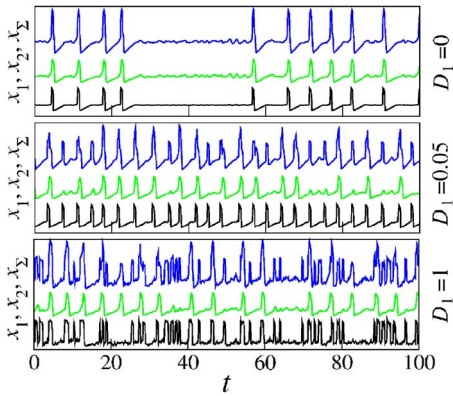


FIG. 2. (Color online) Realizations of x_1 (lower), x_2 (middle), and $x_\Sigma = x_1 + x_2$ (upper trace) of noise-induced oscillations in two coupled FitzHugh-Nagumo systems, Eqs. (1) and (2), for various noise intensities D_1 in the first system for $C=0.07$.

spike slightly more frequently [Fig. 2 ($D_1=0.05$)]. This is reflected by the decrease of respective average ISIs in Fig. 3(a). As D_1 grows further, the mean frequency of spiking in the first subsystem grows in agreement with the theory in Ref. [32]. However, coupling is small here, so the second subsystem only rarely responds with a spike to the spike in the first subsystem. As a result, while the spiking frequency in the first subsystem is further increased, the second subsystem's frequency stays almost constant [Fig. 2 ($D_1=1$) and Fig. 3(a)].

The continuous change of time scales and of coherence of the noise-induced dynamics with D_1 is illustrated in Fig. 3. Here, average ISIs [Fig. 3(a)] and t_{cor} [Fig. 3(b)] are shown. The latter are estimated from x_1 and x_2 , thus quantifying the local dynamics, and from $x_\Sigma = x_1 + x_2$, thus characterizing the global behavior.

All three graphs for t_{cor} show clear maxima which can be regarded as occurrence of coherence resonance (CR) [33].

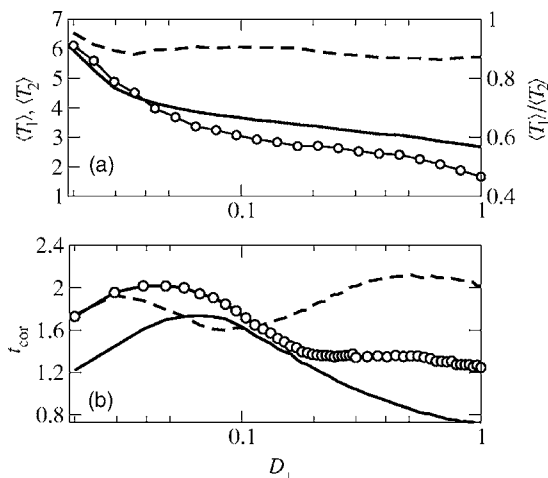


FIG. 3. Time scales and coherence of noise-induced oscillations in two coupled FitzHugh-Nagumo systems, Eqs. (1) and (2), vs D_1 at $C=0.07$. (a) Average ISIs $\langle T_1 \rangle$ (solid line), $\langle T_2 \rangle$ (dashed line), and their ratio (circles). (b) Correlation time t_{cor} obtained from x_1 (solid line), x_2 (dashed line), and x_Σ (circles). See text for details.

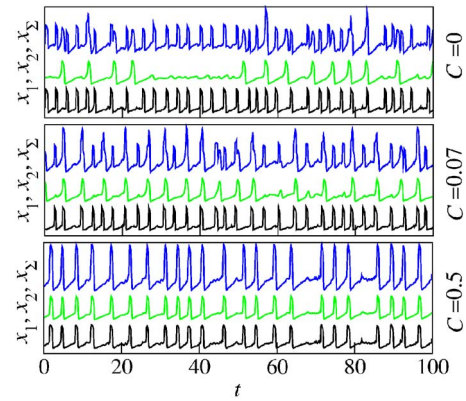


FIG. 4. (Color online) Realizations of x_1 (lower), x_2 (middle), and x_Σ (upper trace) of noise-induced oscillations in two coupled FitzHugh-Nagumo systems, Eqs. (1) and (2), for various coupling strengths C at $D_1=0.25$.

However, in different systems CR occurs at different noise intensities D_1 , and the mutual coupling between the two systems leads to the occurrence of two maxima in t_{cor} calculated from x_2 .

Now consider how noise-induced dynamics changes with variation of the coupling C between neurons. We choose $D_1=0.25$, so that without coupling ($C=0$) the oscillations in the two systems have essentially different time scales with $\langle T_1 \rangle \approx 3.25$ and $\langle T_2 \rangle \approx 8.1$. At $C=0$ the two subsystems oscillate independently (Fig. 4, top panel). As the coupling is increased from zero, the subsystems start to experience each others' influence: each time one system spikes, the other is prompted to spike, too (Fig. 4, middle panel). This results in time scales moving closer [Fig. 3(a)]. As the coupling grows further, the two subsystems spike more simultaneously (Fig. 4, bottom panel), and their average ISIs tend to coincide. The latter can serve as an evidence for stochastic 1:1 frequency synchronization [34], which will be discussed in more detail below.

The full dependence of ISIs and t_{cor} on C is shown in Fig. 5. In the absence of coupling, the two systems randomly oscillate, being independent of each other, hence the coherence of the sum signal is less than the coherences of the individual signals. At large $C > 0.2$, the global coherence becomes equal to the coherence of the second system, which is more ordered individually than its neighbor.

D. Synchronization: frequency (phase) locking and suppression of noise-induced oscillations

Synchronization phenomena in coupled oscillators with noise-induced dynamics were previously considered, e.g., in [34,35]. In contrast to these works, our model consists of essentially nonidentical subsystems whose dynamics is defined by independent sources of noise with different strength, which describes a more general class of natural systems.

In this paper we will discuss only 1:1 synchronization. Since synchronization means an adjustment of time scales in interacting systems, the ratio of their average ISIs would serve as a good tool for its detection. In Fig. 6(a) the ratio

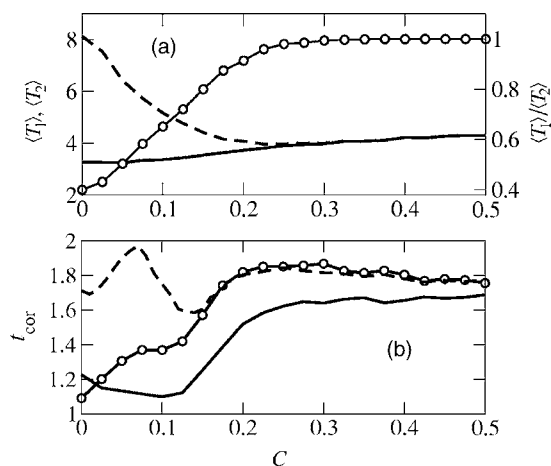


FIG. 5. Time scales and coherence of noise-induced oscillations in two coupled FitzHugh-Nagumo systems, Eqs. (1) and (2), vs coupling strength C at $D_1=0.25$. (a) Average ISIs $\langle T_1 \rangle$ (solid line), $\langle T_2 \rangle$ (dashed line), and their ratio (circles). (b) Correlation time t_{cor} obtained from x_1 (solid line), x_2 (dashed line), and x_Σ (circles). See text for details.

$\langle T_1 \rangle / \langle T_2 \rangle$ is shown for a range of coupling strengths C and of noise intensities D_1 . One can clearly see the 1:1 synchronization region (light area), which has a quite recognizable tongue-like shape, i.e., the larger the coupling strength, the wider the synchronization region with respect to D_1 is.

Next, we explore if phase synchronization accompanies the frequency synchronization. In Fig. 7 the phase difference is shown for $D_1=0.25$: as C is increased from 0.1 to 0.4, the plateaus of $\Delta\varphi_{n,m}(t)$ become longer. At $C=0.4$ the coupling is so strong that the plateau exists (almost) infinitely, which means that the two systems are well 1:1 phase synchronized.

The synchronization index $\gamma_{1,1}$ is computed in the whole range of D_1 and C and is shown in Fig. 6(b). Inside the whole region of 1:1 frequency synchronization where the

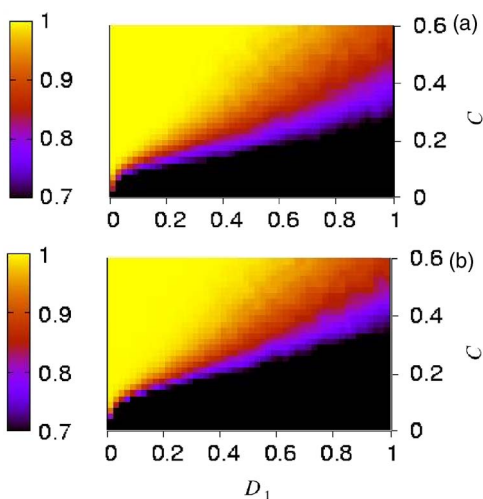


FIG. 6. (Color online) (a) Ratio of average interspike intervals $\langle T_1 \rangle / \langle T_2 \rangle$ from the two systems, and (b) synchronization index $\gamma_{1,1}$ vs the coupling strength C and noise intensity D_1 . The light (yellow) areas roughly outline the 1:1 (a) frequency and (b) phase synchronization tongues.

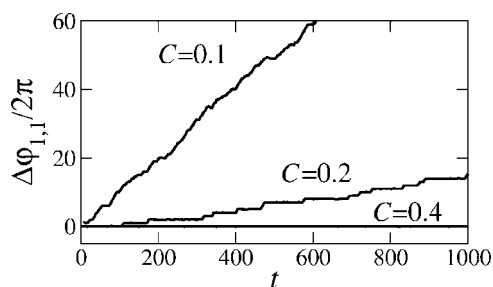


FIG. 7. Phase difference $\Delta\varphi_{1,1}$ for the suspected 1:1 synchronization at three different values of coupling strength C and $D_1=0.25$.

ISI ratio is close to unity, the phase synchronization index is close to unity, too. Thus, phase synchronization occurs together with frequency synchronization.

It has been known for a long time that synchronization can be achieved via at least two different mechanisms, namely *frequency (phase) locking*, and *suppression of natural dynamics*, respectively (see [36] for periodic oscillations and [37] for chaotic and noise-induced oscillations). We found that in our model both these synchronization mechanisms can be realized, depending on how well the time scales of interacting oscillators were separated from each other when uncoupled. An example of synchronization via frequency (phase) locking is illustrated by Fig. 8(a), where for $D_1=0.25$ the spectra of signal x_1 and of x_2 are illustrated for increasing C . As C grows, two distinguishable peaks corresponding to the time scales of the two subsystems move closer and then merge. Figure 8(b) shows how synchronization is realized via the suppression of natural dynamics at $D_1=0.5$. One can see that the increase of C suppresses one of the spectral peaks, i.e., one of the time scales of the system (1). Thus, mutually coupled systems with noise-induced spiking are able not only to demonstrate mutual synchronization itself, but also to reproduce two different synchronization mechanisms, in full analogy with coupled self-oscillating systems.

III. LOCAL DELAYED FEEDBACK CONTROL OF NOISE-INDUCED COOPERATIVE DYNAMICS

In this section we investigate whether the feedback applied only to one of the interacting subsystems, i.e., locally, is able to manipulate the global properties of the system of coupled oscillators. This might simulate a realistic situation where only a small area of the neural network is available for external stimulation. In particular, we will investigate if global time scales, coherence, and the strength of synchronization can be influenced.

The time-delayed feedback control proposed by Pyragas [19] for control of deterministic chaos was previously applied for the control of noise-induced oscillations in a single system with noise-induced dynamics [23–25]. It has been demonstrated that it can successfully change the time scales and coherence of oscillations and is thus a promising tool for control of noise-induced phenomena in general.

For our purpose, we apply the time-delayed feedback to the first subsystem alone, while the second system remains

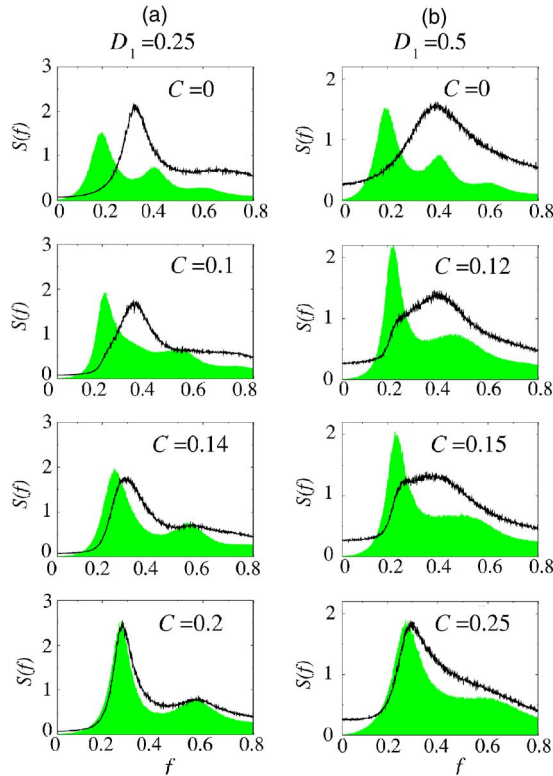


FIG. 8. (Color online) The spectra of x_1 (black) and x_2 (shaded gray area, green online) are compared as the coupling strength C is increased for two different strengths of noise in the first subsystem (a) $D_1=0.25$ and (b) $D_1=0.5$. In (a) the highest spectral peaks move towards each other and coincide: frequency (phase) locking. In (b) the highest peak in the spectrum of x_1 is suppressed, while another peak simultaneously appears and grows at the peak frequency of x_2 : suppression of natural dynamics.

freely coupled to it. The feedback force $F(t)$ is constructed as follows: the slow state variable y_1 is saved at the current time t and at a time $(t-\tau)$, their difference is calculated and multiplied by the feedback strength K . $F(t)$ is then fed back to the y component of the vector field

$$\epsilon_1 \dot{x}_1 = x_1 - \frac{x_1^3}{3} - y_1 + C(x_2 - x_1),$$

$$\dot{y}_1 = x_1 + a + K[y_1(t-\tau) - y_1(t)] + D_1 \xi(t), \quad (7)$$

where τ is the time delay and the other parameters are as in Eqs. (1).

We will be guided by the full picture of cooperative dynamics of the two mutually coupled subsystems that was revealed in Sec. II. We will choose states with different global dynamics by choosing pairs of parameters D_1 and C , and study the effect of the delayed feedback on each state.

We select pairs of points (D_1, C) (see Fig. 6) at which the two systems are (i) far away from $(D_1=0.6, C=0.1)$, (ii) closer to $(D_1=0.6, C=0.2)$, and (iii) almost inside $(D_1=0.15, C=0.2)$ the 1:1 synchronization region. In Sec. III A we study in detail the case of a moderately synchronized

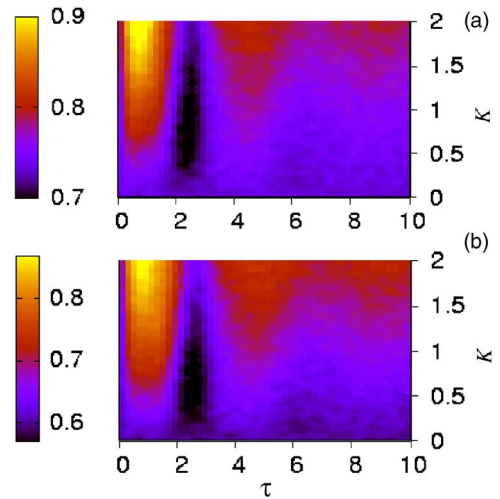


FIG. 9. (Color online) Effect of delayed feedback on frequency and phase synchronization between the two subsystems at $D_1=0.6$ and $C=0.2$, which corresponds to a moderate distance from the 1:1 synchronization tongue shown in Fig. 6. (a) Ratio of average interspike intervals $\langle T_1 \rangle / \langle T_2 \rangle$ from the two systems and (b) synchronization index $\gamma_{1,1}$ vs the control strength K and the time-delay τ .

system at $D_1=0.6$ and $C=0.2$, subject to delayed feedback. We reveal the common features of the feedback effect depending on its parameters τ and K .

Further on, in Sec. III B, we study two more cases of systems further from, and closer to, the 1:1 synchronization region under the delayed feedback action. We compare the effect of the feedback with its effect on a moderately synchronized system.

A. Control of a moderately synchronized system

Here, we consider subsystems Eqs. (7) and (2) with $D_1=0.6$ and $C=0.2$, under the influence of the controlling feedback. We aim to find out if the feedback can make the subsystems more, or less, synchronous, and their global dynamics more or less coherent. In particular, we are interested if perfect 1:1 synchronization can be induced by the local feedback, or if the existing synchronization can be destroyed. The ratio of ISIs and the synchronization index $\gamma_{1,1}$ are shown by color code in Fig. 9 for a large range of the values of the feedback delay τ and strength K . The lighter areas are associated with the stronger 1:1 synchronization, and the values at $K=0$ and at $\tau=0$ characterize the original state of the system without feedback. As seen from Fig. 9, the locally applied delayed feedback is able to move the system's state closer to the 1:1 synchronization with suitable feedback parameters. On the other hand, for $\tau \approx 2.5$ (black area) 1:1 synchronization is suppressed.

An illustration of how realizations x_1 , x_2 , and x_Σ change depending on the feedback strength K as $\tau=1$ is fixed, is given in Fig. 10. Note that the cut at $\tau=1$ (Fig. 9) goes through the region where the strongest 1:1 synchronization is achieved. As K grows, the oscillations in the two subsystems become more and more synchronized until at $K=2$ the two systems start to fire simultaneously almost all the

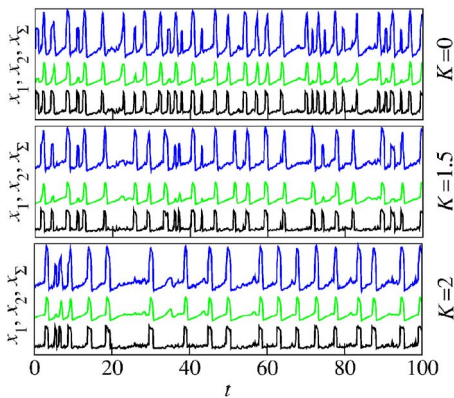


FIG. 10. (Color online) Realizations of x_1 (lower), x_2 (middle), and x_Σ (upper trace) of noise-induced oscillations in two coupled FitzHugh-Nagumo systems, Eqs. (7) and (2) at $D_1=0.6$ and $C=0.2$, subject to delayed feedback with $\tau=1$ for different values of the feedback strength K . See Fig. 11 for reference.

time. However, at least in the given range of K , the perfect 1 : 1 synchronization, with both ISI ratio and synchronization index equal to unity, is still not realized.

Figure 11(a) shows the full dependences upon K of $\langle T_1 \rangle$ (solid line), $\langle T_2 \rangle$ (dashed line), and of their ratio (circles). In Fig. 11(b) the respective dependences of correlation time t_{cor} from x_1 (solid line), x_2 (dashed line), and from the sum signal x_Σ (circles) are given together with the synchronization index $\gamma_{1,1}$ (gray line, green online). Both $\langle T_1 \rangle$ and $\langle T_2 \rangle$ grow monotonically with K , which means that at $\tau=1$ the feedback slows down the oscillations. Within the accuracy of numerical simulation, both ISI ratio and $\gamma_{1,1}$ grow linearly with K , still not achieving the value of 1 at $K=2$. t_{cor} from x_Σ grows with K almost linearly as well, which means that the global

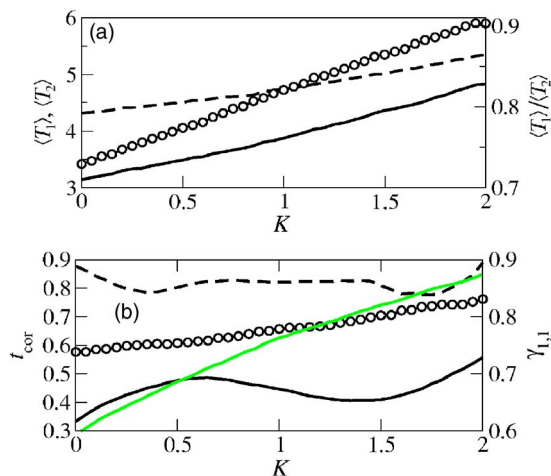


FIG. 11. (Color online) Time scales, coherence, and synchronization index of noise-induced oscillations in two coupled FitzHugh-Nagumo systems, Eqs. (7) and (2), vs K of the local feedback at $\tau=1$, $D_1=0.6$, and $C=0.2$ (see Fig. 9 for reference). (a) Average ISIs $\langle T_1 \rangle$ (solid line) and $\langle T_2 \rangle$ (dashed line), and their ratio (circles). (b) Correlation times t_{cor} obtained from x_1 (solid line), from x_2 (dashed line), and from x_Σ (circles). Synchronization index $\gamma_{1,1}$ (gray line, green online).

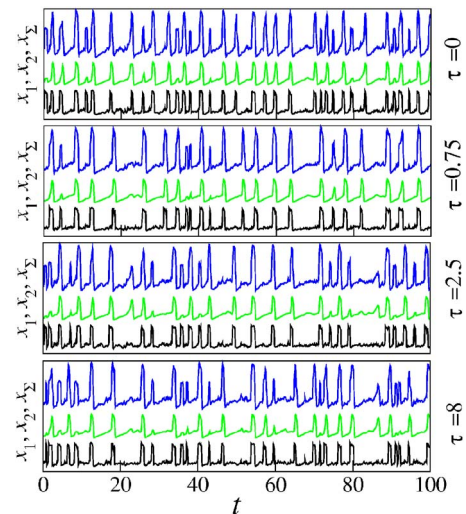


FIG. 12. (Color online) Realizations of x_1 (lower), x_2 (middle), and x_Σ (upper trace) of noise-induced oscillations in two coupled FitzHugh-Nagumo systems, Eqs. (7) and (2), at $D_1=0.6$ and $C=0.2$, subject to delayed feedback with $K=1.5$ for different values of the time delay τ . See Fig. 13 for reference.

dynamics of the system becomes more ordered with the stronger feedback. However, t_{cor} computed from x_1 and x_2 separately are nonmonotonic.

Next, we follow the route with a constant $K=1.5$ that crosses the area with the strongest synchronization, by changing τ . Four respective realizations from the subsystems are shown in Fig. 12. A full picture showing ISIs, their ratio, correlation times, and synchronization index vs τ is given in Fig. 13. Both $\langle T_1 \rangle$ and $\langle T_2 \rangle$, as well as their ratio, change nonmonotonically with τ while its value is smaller than 8. At $\tau > 8$ they start to asymptotically tend to some constant values that are slightly larger than those without feedback.

An increase of τ from zero leads to an increase of both $\langle T_1 \rangle$ and $\langle T_2 \rangle$. But $\langle T_1 \rangle$ grows faster than $\langle T_2 \rangle$, thus their ratio $\langle T_1 \rangle / \langle T_2 \rangle$ grows with τ , as well as the phase synchronization

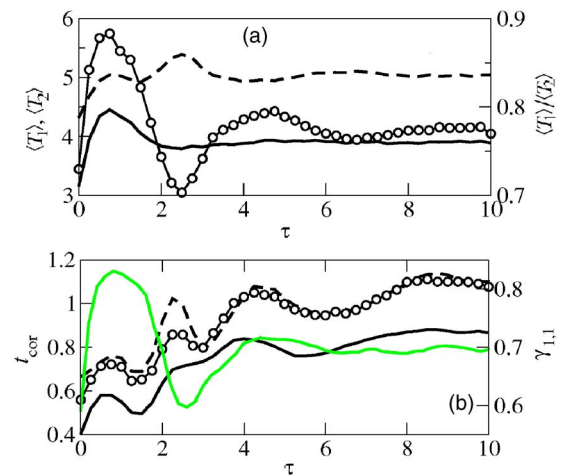


FIG. 13. (Color online) Time scales, coherence, and synchronization index of noise-induced oscillations in two coupled FitzHugh-Nagumo systems, Eqs. (7) and (2), vs time delay τ at $K=1.5$, $D_1=0.6$, and $C=0.2$ (see Fig. 9 for reference). Symbols as in Fig. 11.

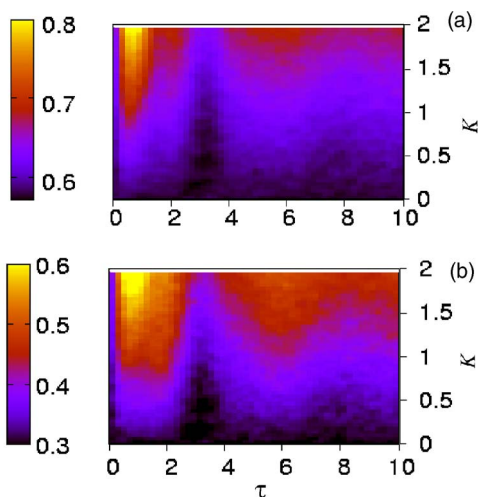


FIG. 14. (Color online) Effect of delayed feedback on frequency and phase synchronization between the two subsystems at $D_1=0.6$ and $C=0.1$, which are further away from the 1:1 synchronization tongue shown in Fig. 6, than those considered in Fig. 9. Plot as in Fig. 9.

index $\gamma_{1,1}$. At the same time, the coherence of each subsystem and of their global dynamics grows, too, as illustrated by the behavior of the respective correlation times t_{cor} [Fig. 13(b)].

After the maximum of $\langle T_1 \rangle$ and $\langle T_2 \rangle$, and of their ratio, is achieved at $\tau \approx 0.7$, both $\langle T_1 \rangle$ and $\langle T_2 \rangle$ start to decrease, but again $\langle T_1 \rangle$ decreases faster than $\langle T_2 \rangle$, thus their ratio decreases. A similar behavior is observed in t_{cor} and in $\gamma_{1,1}$.

Starting from $\tau \approx 2$, the ISI $\langle T_1 \rangle$ of the first system hardly changes with τ . However, counterintuitively, the ISI $\langle T_2 \rangle$ of the second system responds to the further increase of τ by displaying a noticeable maximum at $\tau \approx 2.5$. This leads to a well-pronounced minimum of the ISI ratio [Fig. 13(a)] and of the synchronization index $\gamma_{1,1}$ [Fig. 13(b)]. This phenomenon is accompanied by a respective maximum of the coherence of the second subsystem and of the global dynamics, while neither the time scales nor the coherence of the first subsystem change substantially. This is a highly counterintuitive phenomenon, since the feedback is applied to the first subsystem only, while the second subsystem responds to the changes of the feedback only indirectly through its coupling with the first subsystem.

With the further increase of τ , the dynamics of the second subsystem changes more substantially than the one of the first subsystem, and thus gives a larger contribution to the changes of the global dynamics.

B. Control of a weakly and of a strongly synchronized system

In this subsection we consider subsystems, Eqs. (7) and (2), that are either further from ($D_1=0.6, C=0.1$), or closer to ($D_1=0.15, C=0.2$), the 1:1 synchronization region, under the influence of the controlling feedback.

For $D_1=0.6, C=0.1$, the ratio of ISIs and the synchronization index $\gamma_{1,1}$ are shown by color code in Figs. 14. As

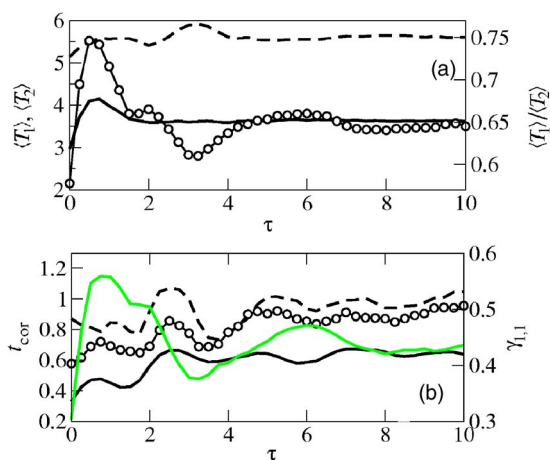


FIG. 15. (Color online) Time scales, coherence, and synchronization index of noise-induced oscillations in two coupled FitzHugh-Nagumo systems, Eqs. (7) and (2), depending on the time delay τ at $K=1.5, D_1=0.6$, and $C=0.1$ (see Fig. 14 for reference). Symbols are as in Fig. 11.

with the stronger synchronized subsystems, the feedback is able to move the whole system towards a more synchronous state.

As with the example of Sec. III A, we consider the cut of the τ - K plane along $K=1.5$, choosing the route that goes through the lighter area of the largest synchronization index. ISIs, their ratio, correlation times, and synchronization index are shown in Fig. 15 depending on τ . Their behavior has some similarities to that in a moderately synchronized system of Sec. III A.

Namely, the initial increase of τ from zero leads to the growth of both $\langle T_1 \rangle$ and $\langle T_2 \rangle$, the former growing faster than the latter. This leads to the growth of the ISI ratio and of synchronization index $\gamma_{1,1}$, and also of t_{cor} of x_1 and of x_S . All variables achieve the maximum at $\tau \approx 0.6$. After that, all the variables describing the first system start to decrease, while $\langle T_2 \rangle$ does not change until $\tau=1.5$. Here, the ISI ratio decreases correspondingly, like for $C=0.2$. And again, after $\tau=2$, $\langle T_1 \rangle$ hardly changes with τ , while $\langle T_2 \rangle$ exhibits a noticeable maximum that leads to the rapid drop of both ISI ratio and synchronization index.

With further increase of τ beyond 6, both subsystems respond only slightly and comparably to the changes in τ .

Note that either for a moderately synchronized system, or for a system that is less synchronized, the feedback is able to make 1:1 synchronization substantially stronger for a suitable choice of its parameters. However, it cannot destroy the existing synchronization or weaken it as much as it can strengthen it.

For the system that is very well synchronized from the beginning at $D_1=0.15$ and $C=0.2$ with $\gamma_{1,1}=0.99$, we reveal the ISI ratio and synchronization index $\gamma_{1,1}$ for a large range of K and τ (Fig. 16). Already this picture shows that delayed feedback can either enhance or suppress synchronization.

For a more detailed picture of the phenomena induced by the feedback, a cut of this picture along $K=1$ is given in Fig. 17 where the ISIs and their ratio are shown, together with $\gamma_{1,1}$ and correlation times for x_1, x_2 , and x_S . An immediate

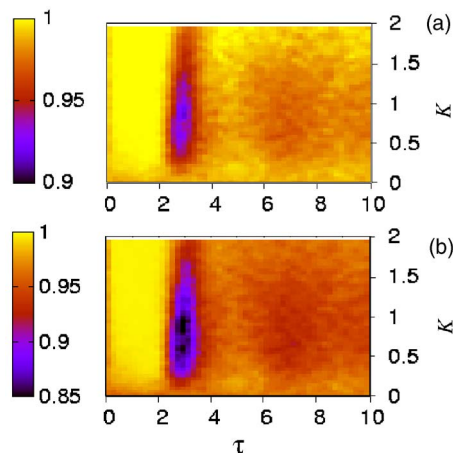


FIG. 16. (Color online) Effect of delayed feedback on frequency and phase synchronization between the two subsystems at $D_1 = 0.15$ and $C = 0.2$, which are closer to the 1:1 synchronization tongue shown in Fig. 6, than those considered in Fig. 9. Plot as in Fig. 9.

obvious observation is that, in contrast to the two previously considered cases of less synchronous subsystems, here the feedback can make synchronization perfect with $\gamma_{1,1} = 1$, and can maintain it like this for a substantial range of $\tau \in [0.25; 2]$ [Fig. 17(a)]. The fact that the two subsystems are very synchronous from the beginning is also supported by very similar values of the correlation times of both systems' realizations and of their sum at $\tau = 0$ [Fig. 17(b)].

As τ is slightly increased from zero, as in the two previous examples, both $\langle T_1 \rangle$ and $\langle T_2 \rangle$ grow. But, as before, $\langle T_1 \rangle$ grows a little faster than $\langle T_2 \rangle$. This can hardly be resolved in the plots, since $\langle T_1 \rangle$ and $\langle T_2 \rangle$ are very close and hardly distinguishable. However, the difference between them, and the disappearance of this difference, is visible through the ISI ratio [Fig. 17(a)].

With this, t_{cor} and $\gamma_{1,1}$ slightly grow, too. All quantities considered achieve their maxima at $\tau \approx 0.25$. After that, as τ

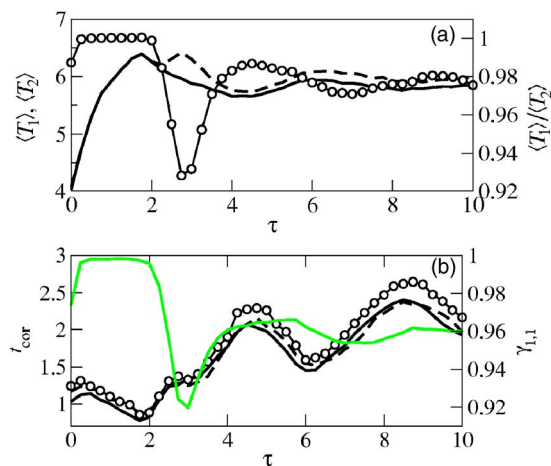


FIG. 17. (Color online) Time scales, coherence, and synchronization index of noise-induced oscillations in two coupled FitzHugh-Nagumo systems, Eqs. (7) and (2), depending on the time delay τ at $K = 1$, $D_1 = 0.15$, and $C = 0.2$ (see Fig. 16 for reference). Symbols as in Fig. 11.

increases, the individual ISIs $\langle T_1 \rangle$ and $\langle T_2 \rangle$ grow simultaneously and remain equal, so that their ratio and synchronization index $\gamma_{1,1}$ stay equal to 1 with high accuracy in the range $\tau \in [0.25; 2]$.

However, surprisingly, while the ISI ratio and $\gamma_{1,1}$ are equal to 1, i.e., the subsystems maintain the same level of perfect synchrony, all three correlation times decrease with τ . This means that while the two subsystems fire simultaneously, these firings occur less regularly. Thus, the feedback here can introduce disorder into the system without destroying its perfect synchronization.

Then, as τ continues to increase beyond the value of 2, as in the previous examples, the second subsystem demonstrates a noticeable maximum of its ISI $\langle T_2 \rangle$. Although unlike in the two other examples, here $\langle T_1 \rangle$ continues to decrease, the ISI ratio and $\gamma_{1,1}$ exhibit a sharp minimum, and then grow again.

At τ increases beyond 8, the ISI ratio and $\gamma_{1,1}$ become less and less dependent on τ , asymptotically tending to some values that are only slightly lower than without the feedback. On the contrary, t_{cor} continues to change nonmonotonically with τ , never becoming less than without the feedback. Since the system is in the state of a strong synchronization throughout the changes in τ , the changes in all three curves t_{cor} occur synchronously.

Thus, the feedback can make both local and global dynamics of the system more coherent, and at the same time weaken synchronization.

IV. SUMMARY AND CONCLUSIONS

We have considered a model describing two coupled excitable neurons, in the form of two mutually coupled non-identical excitable FitzHugh-Nagumo systems, subject to independent sources of noise with different strengths. In order to assess the effect of time-delayed feedback control upon the coupled system, we have analyzed the following characteristics: the time scales of the individual systems quantified as mean interspike intervals (ISI); the ISI ratio as a measure of frequency synchronization; the coherence quantified by the correlation time of the individual subsystems' realizations and of their sum; and the index of 1:1 phase synchronization between the subsystems.

The coupled system without control displays a 1:1 synchronization tongue in the (D_1, C) parameter plane, given by the noise strength D_1 in the first subsystem and the coupling strength C . Interestingly, frequency and phase synchronization occurred in the same area of the parameter plane.

Two mechanisms for synchronization were identified: phase (frequency) locking, and suppression of natural dynamics, respectively.

Next, the first of the two interacting subsystems was subjected to the local delayed feedback with the aim to manipulate the global dynamics of the system of interacting oscillators. The feedback force was constructed as a difference between the current state of the system and its state some τ time units before, multiplied by a positive constant K .

The delayed feedback was applied to the system in three states of synchrony: moderately synchronized, weakly syn-

chronized, and strongly synchronized. In all three cases, 1:1 synchronization could be either improved or weakened, depending upon the choice of τ and K . Like the correlation times, the synchronization index is modulated nonmonotonically as a function of the delay time τ , indicating that there is resonancelike behavior for certain values of τ . Perfect synchronization can only be achieved if the uncontrolled state is already sufficiently synchronized.

The mechanism behind the reported action of the delayed feedback is as follows. As it was shown earlier [23,24], the feedback applied to a single excitable system is able to change the time scales and coherence of noise-induced oscillations. When the system subjected to the feedback is coupled to another system, the shift of the time scale of the former will lead to a proportional shift of the time scale of the latter. The exact magnitude of the shift in the second subsystem will depend on the closeness of the two subsystems to the state of synchronization. Only if the two subsystems are sufficiently 1:1 synchronized from the beginning, the shift in the second system can be expected to match the shift in the first system.

Interestingly, the above mechanism does not always work in the system considered. Namely, for some ranges of time delay τ , the change in τ does not cause any noticeable change in the system to which the feedback is applied. However, it does change the properties of oscillations in the system that is coupled to it, albeit that does not experience the influence of the feedback directly.

An important observation is that the delay-induced increase of coherence of the global dynamics is most frequently accompanied by the growth of the degree of synchronization. However, a high synchronization index does not always mean high coherence: delayed feedback can induce, or make stronger, the synchronization between the two subsystems, but the state of each subsystem, and their global dynamics, can become more disordered at the same time. The converse is also true.

It is remarkable that delayed feedback control can influence global characteristics of the two coupled neurons although the control is only applied locally to a subsystem. We were able to enhance or destroy the regularity of oscillations and the stochastic synchronization of the two neurons by choosing appropriate control parameters, in particular a suitable delay time.

We consider these findings as important for the understanding of coupled nonlinear systems and see possible applications especially in neuroscience.

In fact, experimental studies of two coupled neurons from the stomatogastric ganglion of a lobster [29], and from a leech [30] have reported various degrees of synchrony of excitatory postsynaptic potentials. As stochastic sources of the spontaneous random firing of neurons, noise due to the conducting ion channels, synaptic noise, and noise resulting from the coupling to a large number of other neurons emitting signals, have been identified [38]. Also it was demonstrated experimentally [6] that spatially and temporally coherent Ca^{2+} waves, mediated by network noise, may play an important role in generating correlated neural activity. By applying delayed feedback control to real neural systems one should be able to influence neural synchrony. First results of applying time-delayed neurofeedback from real-time magnetoencephalography (MEG) signals to humans via visual stimulation in order to suppress the alpha rhythm, which is observed due to strongly synchronized neural populations in the visual cortex in the brain, look promising [39]. Further work should focus on more sophisticated models and on coupling more than two neurons.

ACKNOWLEDGMENTS

This work was partially supported by DFG in the framework of Sfb 555 (complex nonlinear processes). B.H. thanks the Studienstiftung des deutschen Volkes for support and gratefully acknowledges the hospitality of Loughborough University. A.B. acknowledges the support of EPSRC (UK).

-
- [1] H. A. Braun, H. Wissing, K. Schäfer, and M. C. Hirsch, *Nature* (London) **367**, 270 (1994).
 - [2] J. Lu and H. M. Fishman, *Biophys. J.* **69**, 2458 (1995).
 - [3] V. M. Eguiluz, M. Ospeck, Y. Choe, A. J. Hudspeth, and M. O. Magnasco, *Phys. Rev. Lett.* **84**, 5232 (2000).
 - [4] W. R. Softky and C. Koch, *J. Neurosci.* **13**, 334 (1993).
 - [5] A. L. Hodgkin and A. F. Huxley, *J. Physiol.* (London) **117**, 500 (1952).
 - [6] P. Jung, A. Cornell-Bell, K. S. Madden, and F. Moss, *J. Neurophysiol.* **79**, 1098 (1998).
 - [7] M. Badoual, M. Rudolph, Z. Piwkowska, A. Destexhe, and T. Bal, *Neurocomputing* **65**, 493 (2005).
 - [8] X.-J. Wang, *Neuroscience* **59**, 21 (1994).
 - [9] A. Neiman and D. F. Russell, *Phys. Rev. Lett.* **86**, 3443 (2001).
 - [10] J. M. Samonds, J. D. Allison, H. A. Brown, and A. B. Bonds, *Proc. Natl. Acad. Sci. U.S.A.* **101**, 6722 (2004).
 - [11] A. Benucci, P. F. M. J. Verschure, and P. König, *Phys. Rev. E* **70**, 051909 (2004).
 - [12] P. Tass, M. G. Rosenblum, J. Weule, J. Kurths, A. Pikovsky, J. Volkmann, A. Schnitzler, and H.-J. Freund, *Phys. Rev. Lett.* **81**, 3291 (1998).
 - [13] P. Grosse, M. J. Cassidy, and P. Brown, *Clin. Neurophysiol.* **113**, 1523 (2002).
 - [14] E. Ott, C. Grebogi, and J. A. Yorke, *Phys. Rev. Lett.* **64**, 1196 (1990).
 - [15] *Handbook of Chaos Control*, edited by H. G. Schuster (Wiley-VCH, Weinheim, 1999).
 - [16] S. Boccaletti, C. Grebogi, Y. C. Lai, H. Mancini, and D. Maza, *Phys. Rep.* **328**, 103 (2000).
 - [17] M. Rosenblum and A. Pikovsky, *Phys. Rev. E* **70**, 041904 (2004).
 - [18] O. V. Popovych, C. Hauptmann, and P. A. Tass, *Phys. Rev. Lett.* **94**, 164102 (2005).
 - [19] K. Pyragas, *Phys. Lett. A* **170**, 421 (1992).
 - [20] N. Baba, A. Amann, E. Schöll, and W. Just, *Phys. Rev. Lett.*

- 89**, 074101 (2002).
- [21] O. Beck, A. Amann, E. Schöll, J. E. S. Socolar, and W. Just, *Phys. Rev. E* **66**, 016213 (2002).
- [22] J. Unkelbach, A. Amann, W. Just, and E. Schöll, *Phys. Rev. E* **68**, 026204 (2003).
- [23] N. B. Janson, A. G. Balanov, and E. Schöll, *Phys. Rev. Lett.* **93**, 010601 (2004).
- [24] A. G. Balanov, N. B. Janson, and E. Schöll, *Physica D* **199**, 1 (2004).
- [25] J. Pomplun, A. Amann, and E. Schöll, *Europhys. Lett.* **71**, 366 (2005).
- [26] G. J. Escalera Santos, J. Escalona, and P. Parmananda, *Phys. Rev. E* **73**, 042102 (2006).
- [27] B. Lindner, J. García-Ojalvo, A. Neiman, and L. Schimansky-Geier, *Phys. Rep.* **392**, 321 (2004).
- [28] D. T. J. Liley and J. J. Wright, *Network Comput. Neural Syst.* **5**, 175 (1994).
- [29] R. D. Pinto, P. Varona, A. R. Volkovskii, A. Szücs, H. D. I. Abarbanel, and M. I. Rabinovich, *Phys. Rev. E* **62**, 2644 (2000).
- [30] F. F. De-Miguel, M. Vargas-Caballero, and E. Garcia-Perez, *J. Exp. Biol.* **204**, 3241 (2001).
- [31] M. G. Rosenblum, A. S. Pikovsky, J. Kurths, C. Schäfer, and P. Tass, in *Handbook of Biological Physics* edited by F. Moss and S. Gielen (Elsevier Science, Amsterdam, 2001), Vol. 4, Ch. 9, pp. 279–321.
- [32] B. Lindner and L. Schimansky-Geier, *Phys. Rev. E* **60**, 7270 (1999).
- [33] A. S. Pikovsky and J. Kurths, *Phys. Rev. Lett.* **78**, 775 (1997).
- [34] S. K. Han, T. G. Yim, D. E. Postnov, and O. V. Sosnovtseva, *Phys. Rev. Lett.* **83**, 1771 (1999).
- [35] D. E. Postnov, O. V. Sosnovtseva, S. K. Han, and W. S. Kim, *Phys. Rev. E* **66**, 016203 (2002).
- [36] P. Landa, *Self-oscillations in the Systems with Finite Number of Degree of Freedom* (Nauka, Moscow, 1980) (in Russian).
- [37] E. Mosekilde, Yu. Maistrenko, and D. Postnov, *Chaotic Synchronization. Applications to Living Systems* (World Scientific, Singapore, 2000), Series A, Vol. 42.
- [38] S. Zeng and P. Jung, *Phys. Rev. E* **70**, 011903 (2004).
- [39] V. Hadamschek, Ph.D. thesis, TU Berlin, 2006 (unpublished).